SAND2014-17637C

Calculating the Impact Force of Supersonic Hail Stones Using SWAT-TEEM

Tyler F. Schoenherr
Experimental Mechanics, NDE and Model Validation Department
Sandia National Laboratories[1]
P.O. Box 5800 - MS0557
Albuquerque, NM, 87185

Abstract

In the aerospace industry, hail strikes on a structure are an environment that must be considered when qualifying a product. Performing a physical test on a product would require a test setup that would launch a fabricated hail stone at an expensive prototype. This test may be difficult or impossible to execute and destructive to the product. Instead of testing, a finite element model (FEM) may be used to simulate the damage and consequences of a hail strike. In order to use a FEM in this way, an accurate representation of the input force from a hail stone must be known. The purpose of this paper is to calculate the force that a hail stone imparts on an object using the inverse method SWAT-TEEM. This paper discusses the advantages of using SWAT-TEEM over other force identification methods and exercises the algorithm for a test series of hail strikes that include multiple angles of attack and multiple velocities which include speeds that are supersonic.

Keywords
Hail, Force, Impact, SWAT, Ice

Introduction

Aerospace systems experience a variety of unique inputs ranging from aerodynamic loading to turbine induced vibration. The possibility of hail strikes on the system is a viable mechanical input to the system and must be analyzed when qualifying the system for its intended function. To determine if the system will survive the hail strike, a test is run either analytically or experimentally. If the system is qualified experimentally, then a test is run that fires a hail stone at the system and hits it in the location that causes the most damage to determine if the system will survive. However, firing a hail stone accurately at the known worst case location is difficult and expensive to execute. Also, the test may be destructive and most hardware is too costly or is one of a kind. The test would still not determine if the system could survive in a hail storm with multiple consecutive hail strikes.

Because of the difficulties of an experimental test, an analytical or finite element model is typically utilized. In order to properly use a calibrated finite element model, an accurate representation of the force is needed as an input to the

[1]Sandia National Laboratories is a multi-program laboratory managed and operated by Sandia Corporation, a wholly owned subsidiary of Lockheed Martin Corporation, for the U.S. Department of Energys National Nuclear Security Administration under contract DE-AC04-94AL85000

model. To determine the force that a hail strike imparts on a system, characterization tests have to be performed that measure or calculate the force that a hail stone imparts on an object.

This characterization has been attempted in the past using different methods. Force gauges have directly been used to measure the force that the hail stone imparts on a plate [7][5]. This method works for normal impacts and low frequency strikes, but force piezo electric gauges typically have low internal resonances and have issues measuring shear forces or moments if the strike is not perfectly normal. This would make measuring the force of high speed or glancing hail strikes hard to measure with this method.

Another method to measure the force a hail stone imparts on a surface has been proposed by Tippmann et al. [8]. They proposed to shoot the hail stone into a long cylindrical rod instrumented with strain gauges. The strain measured could be related to stress and the force with knowledge of the geometry of the rod. This process is very similar to a traditional Hopkinson bar test.

This paper presents another alternative to calculating the force imparted by a hail stone. The SWAT-TEEM (Sum of Weighted Accelerations Technique-Time Eliminated Elastic Motion) is the algorithm in this paper that is used to calculate the the hail force. The SWAT algorithm developed by Gregory et al. [3] was later used to calculate the input forces on a system by Carne et al. [2]. Later, the algorithm was modified to use the time domain responses for the inversion instead of the mode shape and was renamed to SWAT-TEEM [6]. Both of these algorithms calculate the sum of the forces and moments from responses at the center of gravity.

Both SWAT and SWAT-TEEM algorithms are considered in this paper to calculate the hail impact forces. To determine which algorithm would be used, a characterization test is run. This test measures the mode shapes of the system for the SWAT algorithm. Because the characterization test involves hitting the object with a force gauge on a hammer, it provides a truth test to compare the results from SWAT and SWAT-TEEM to a measured hammer force. This truth test provides data to determine which algorithm to use for the hail impact test and provides evidence for the determination of the useful bandwidth of the calculated force.

Forces from hail impacting an aluminum plate are the interest of this paper. In addition to calculating the force of a hail stone impacting an aluminum plate at a normal angle, normal forces will be calculated for hail stones at different impact angles and at different speeds. This includes the forces of hail stones that are traveling at supersonic speeds. The paper concludes with the examination of all of the calculated forces and their corresponding angles.

Force Reconstruction Theory

Force reconstruction is used to describe the inverse problem where the system's dynamic properties and response to a force is known. From the system's equations of motion,

$$\bar{X}(\omega) = \mathbf{H} \cdot \bar{F}(\omega), \tag{1}$$

where $\bar{F}$ is the input force, $\mathbf{H}$ is the system's dynamic properties, and $\bar{X}$ is the system's response from the input force, the system's dynamic properties can be inverted to calculate the input force on that system that caused the measured response as shown in

$$\mathbf{H}^{-1} \cdot \bar{X}(\omega) = \bar{F}(\omega). \tag{2}$$

Although the inversion process appears straightforward, Eq 2 typically fails due to the $\mathbf{H}$ matrix being ill conditioned. It is ill conditioned because the solution for the force matrix is generally not unique. Also, the $\mathbf{H}$ matrix is generally rank deficient for some frequency lines, so it cannot be accurately inverted. The following subsections present two algorithms that solve this inverse problem. These algorithms are dubbed SWAT algorithms and they solve the non-uniqueness problem by reducing the force vector size down to six. The six vectors represent the sum of the forces and moments acting at the center of gravity which yields a unique solution.

Formulation of SWAT (Sum of Weighted Acceleration Technique)

The derivation of the SWAT algorithm that is used to calculate the sum of the external forces begins with the 2nd order linear equations of motion,

$$\mathbf{M}\ddot{\bar{x}} + \mathbf{C}\dot{\bar{x}} + \mathbf{K}\bar{x} = \bar{F}, \tag{3}$$

where $\mathbf{M}$ is the mass matrix, $\mathbf{C}$ is the damping matrix and $\mathbf{K}$ is the stiffness matrix of the system. Modal substitution is then used to estimate the physical response with modal degrees of freedom shown by

$$\boldsymbol{\phi}\bar{q} \approx \bar{x}, \tag{4}$$

where $\boldsymbol{\phi}$ is the mode shapes of the system and $\bar{q}$ is the generalized modal coordinates. The modal approximation shown in Eq 4 is substituted into Eq 3 to get

$$\mathbf{M}\boldsymbol{\phi}\ddot{\bar{q}} + \mathbf{C}\boldsymbol{\phi}\dot{\bar{q}} + \mathbf{K}\boldsymbol{\phi}\bar{q} = \bar{F}. \tag{5}$$

At this point, Eq 5 is premultiplied by the transpose of the rigid body modes to get

$$\phi_r^T\mathbf{M}\boldsymbol{\phi}\ddot{\bar{q}} + \phi_r^T\mathbf{C}\boldsymbol{\phi}\dot{\bar{q}} + \phi_r^T\mathbf{K}\boldsymbol{\phi}\bar{q} = \phi_r^T\bar{F}. \tag{6}$$

Because there is no internal damping or internal stiffness forces for the rigid body degrees of freedom, Eq 6 simplifies to

$$\phi_r^T\mathbf{M}\boldsymbol{\phi}\ddot{\bar{q}} = \phi_r^T\bar{F} \tag{7}$$

due to

$$\phi_r^T\mathbf{C} = 0 \;\&\; \phi_r^T\mathbf{K} = 0. \tag{8}$$

The physical degrees of freedom are substituted for the modal degrees of freedom using the relationship in Eq 4 into Eq 7 to get

$$\phi_r^T\mathbf{M}\ddot{\bar{x}} = \phi_r^T\bar{F}. \tag{9}$$

Each row of Eq 9 shows that the weighted sum of the measured accelerations can be equates to the sum of the external forces on the test object for a specific direction. The weights are represented by a linear combination of the mass matrix. The mass matrix is orthogonal with respect to the mode shapes as shown by

$$\phi_r^T\mathbf{M}\phi = [M_r\ 0]. \tag{10}$$

The mode shape matrix which includes both rigid body and elastic mode shapes is inverted and multiplied by both sides of Eq 10 to get

$$\phi_r^T\mathbf{M} = [M_r\ 0]\phi^+ \tag{11}$$

where the superscript + denotes the pseudo-inverse of the matrix. Equation 11 is substituted back into Equation 9 to get

$$[M_r\ 0]\phi^+\ddot{\bar{x}} = \phi_r^T\bar{F}. \tag{12}$$

Equation 12 shows that the sum of the weighted accelerations can be used to calculate the sum of the external forces. These forces are the sum of the forces in the three principal translational directions that act at the center of gravity and the three moments around those three principal axes. The weights for the accelerations are the mass properties of the test object multiplied with the rigid body vector components of the pseudo-inverse of the mode shape matrix that includes rigid body and elastic mode shapes.

Formulation of SWAT-TEEM (Sum of Weighted Acceleration Technique - Time Eliminated Elastic Modes)

The derivation of the SWAT-TEEM algorithm utilizes the same beginning steps as SWAT until Eq 9. At this point a weighting vector, w, is defined as

$$w^T = \phi_r^T \mathbf{M}. \tag{13}$$

and substituted into Eq 9 to obtain

$$w^T \ddot{\bar{x}} = \phi_r^T \bar{F}. \tag{14}$$

To solve for the weighting vector, an assumption of the input force is made. In the case where the structure is impacted by an external force and then in a free state, there are no external forces after impact and the accelerations of the system would be in an exponential decay and Eq 14 after the impact simplifies to

$$w^T \ddot{\bar{x}} = 0. \tag{15}$$

To obtain a non-trivial solution, information about the rigid body modes need to be included because they were not present in the free decayed response. The rigid body constraint is formed by post-multiplying Eq 13 by the rigid body shapes to get

$$w^T \phi_r = \phi_r^T \mathbf{M} \phi_r, \tag{16}$$

which can be simplified to

$$w^T \phi_r = M_r. \tag{17}$$

Equation 17 is added to Eq 15 to get

$$w^T \left[\phi_r \ \ddot{\bar{x}}\right] = \left[M_r \ 0\right]. \tag{18}$$

Equation 18 is solved for the six weighting vectors in a constrained least squares problem with the rigid body term being the constraint. The pseudo-inverse of the rigid body shapes and the responses of the free decayed response are multiplied by both sides to solve for the weighting vector. These weight vectors are then substituted back into Equation 14 to solve the for the external forces. Because the pseudo-inverse includes the time domain response of the system which are a linear combination of the mode shapes, the mode shapes of the system do not need to be separately calculated.

Condition of the Inverse in SWAT and SWAT-TEEM

The SWAT algorithm inverts the mode shape matrix as shown in Eq 11. Since the response matrix must be inverted, one must be sure that it is not rank deficient, so there must be at least as many sensors as modes in the bandwidth of interest. The inversion of the mode shape matrix has to be well conditioned to avoid error in the computation. The condition number of the mode shape matrix is controlled through examination of the mode shapes and placing accelerometers in a way that the accelerometers span of the space of the mode shapes. This could be done by over instrumenting a modal test or using a finite element model to place accelerometers to minimize the condition of the shapes.

SWAT-TEEM inverts the rigid body mode shapes and the time response of a freely decaying signal after impact. Although the algorithm does not directly invert the mode shapes, the algorithm inverts the responses which contain a linear combination of all the modes excited by the forcing function. Therefore, SWAT-TEEM also needs to have the instrumentation span the space of all mode shapes that are active in the bandwidth of the forcing function.

Test Item Description

The test article was an 7075 aluminum plate. The dimensions of the plate were 12”×11”×2” and a photograph of the back side of the plate instrumented for the hail impact test can be found in Figure 1. Twenty one 1/4” holes were drilled and tapped at the measured locations so that the instrumentation could be screwed at the desired measured locations. The coordinates of the nodes used in both the characterization and hail impact tests are given in Table 1. The node locations were chosen by checking the condition number of the mode shape matrix calculated by a FEM at candidate locations to ensure that the instrumentation produces a full rank matrix. The weight of this plate in this configuration without gauges, wires or tape was 26.497 lbs. Figure 1 also shows the direction of the X and Y axes. The Z axis is a resultant of the X and Y axes with respect to the right hand rule. The origin of the coordinate system is at the geometric center of the plate.

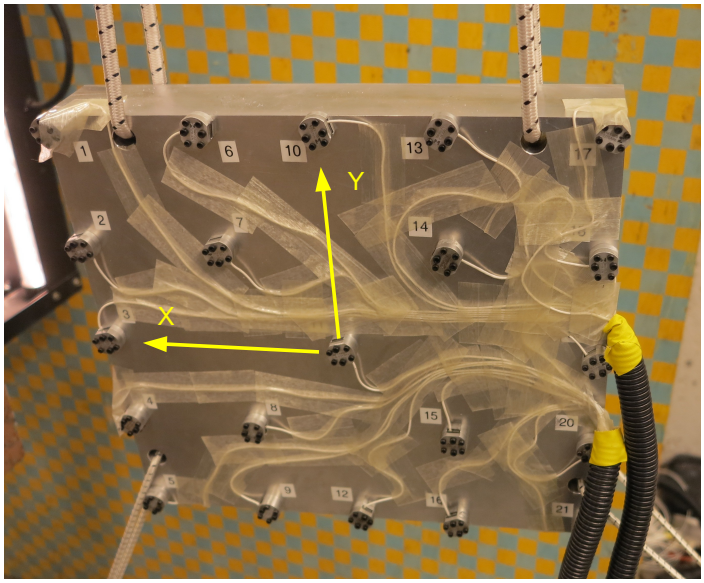

Figure 1: Photo of the plate’s nodes and coordinate system

Table 1: Coordinates for the Plate Nodes

Node	Coordinate System	Coordinates			Node	Coordinate System	Coordinates		
		X (in)	Y(in)	Z (in)			X (in)	Y(in)	Z (in)
1	Cartesian	5.75	5.25	-1.25	12	Cartesian	0.00	-5.25	-1.25
2	Cartesian	5.75	2.50	-1.25	13	Cartesian	-2.50	5.25	-1.25
3	Cartesian	5.75	0.00	-1.25	14	Cartesian	-2.50	2.50	-1.25
4	Cartesian	5.75	-2.50	-1.25	15	Cartesian	-2.50	-2.50	-1.25
5	Cartesian	5.75	-5.25	-1.25	16	Cartesian	-2.50	-5.25	-1.25
6	Cartesian	2.50	5.25	-1.25	17	Cartesian	-5.75	5.25	-1.25
7	Cartesian	2.50	2.50	-1.25	18	Cartesian	-5.75	2.50	-1.25
8	Cartesian	2.50	-2.50	-1.25	19	Cartesian	-5.75	0.00	-1.25
9	Cartesian	2.50	-5.25	-1.25	20	Cartesian	-5.75	-2.50	-1.25
10	Cartesian	0.00	5.25	-1.25	21	Cartesian	-5.75	-5.25	-1.25
11	Cartesian	0.00	0.00	-1.25					

Characterization Test

The purpose of the characterization test was to experimentally measure the elastic mode shapes of the aluminum plate for the SWAT analysis. Its other purpose was to compare the SWAT and SWAT-TEEM forces to a measured hammer force to determine the algorithms' accuracy. Three rigid body forces were measured and calculated from this analysis. The three rigid body forces that were calculated were the force in the Z direction, the moment about the Y axis and the moment about the X axis.

The analysis during the characterization portion of this test series consisted of fitting modal parameters to the data so that the mode shapes could be used for SWAT. Also, because a measured force was applied to the plate, a validation test of SWAT and SWAT-TEEM was run to validate the Matlab code and determine the frequency band limitation of the algorithms by comparing the reconstructed forces to the measured force. All of the modal parameters fit from the data used the Synthesize Modes and Correlate (SMAC) algorithm developed by Hensley and Mayes [4].

Figure 2 shows the SWAT and SWAT-TEEM reconstructed forces in the Z direction against the hammer strike in the Z direction. These reconstructions can be examined in the frequency domain in Figure 3. In the frequency domain, it was noted that SWAT-TEEM was an excellent representation of the force up to 9000 Hz and performed better than SWAT which was an excellent representation of the force up to 4000 Hz. This cutoff frequency was chosen because the quality of the reconstruction degraded past 10 kHz because the instrumentation did not span the space of the motion past 10kHz. Therefore, SWAT-TEEM was the algorithm used in the hail impact test.

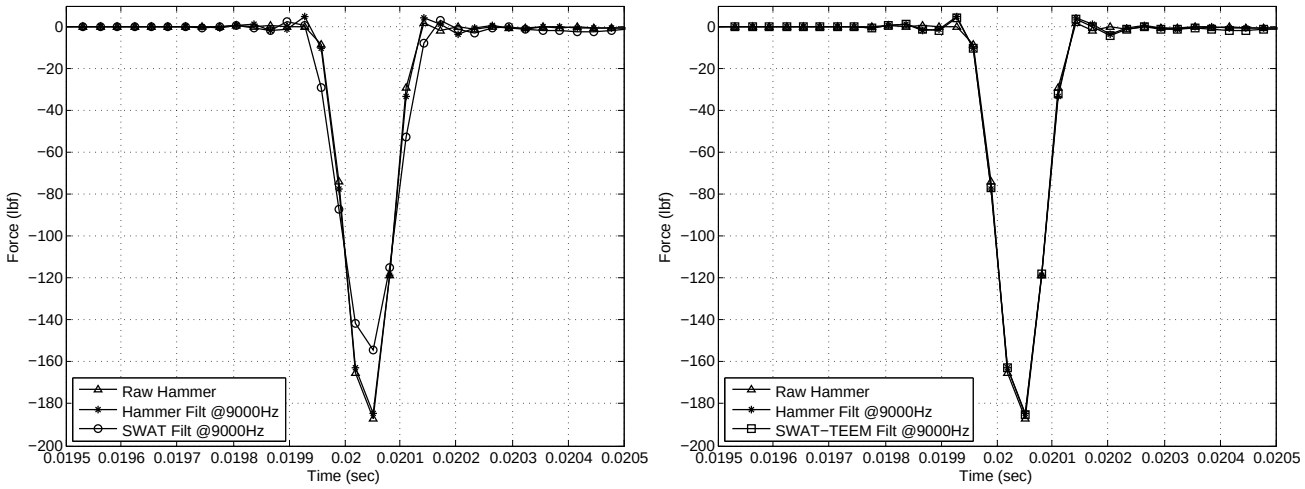

Figure 2: Reconstructed SWAT (Left) and SWAT-TEEM (Right) force compared to the hammer hit

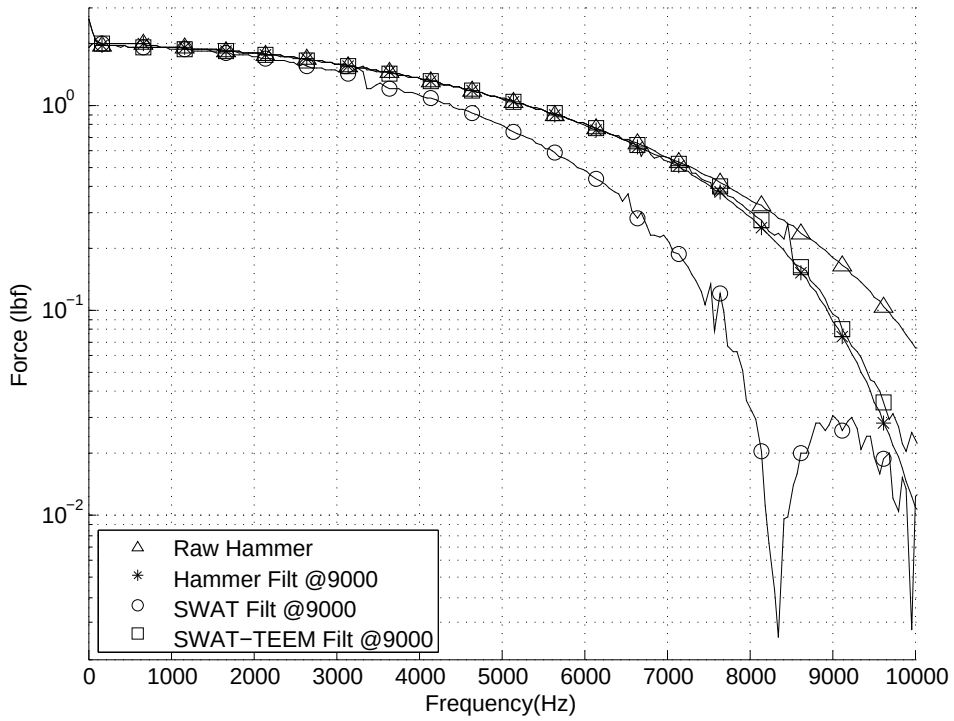

Figure 3: Reconstructed forces compared to the hammer hit in frequency domain

Another check on the validity of the reconstructed forces would be to calculate the location of the hammer hit by dividing the reconstructed moments by the reconstructed force to get the moment arm distance from the center of gravity of the plate. The moment arms were calculated using the force and moments at the time of the peak force. The calculated moment arms were 0.002 inches in the X direction and 0.016 inches in the Y direction. The hammer hit was located at node 11, which had coordinates of approximately (0,0).

Although the characterization test and hail impact test measured three rigid body forces, it was possible to measure all six rigid body forces. This would require more instrumentation to span the space of the in plane rigid body and elastic modes. This would provide input on the tangential forces that were caused by a hail stone. This was not done for this test series due to the lack of resources in instrumentation and data acquisition channels.

Hail Impact Test

The purpose of this test was to characterize the force of a hailstone striking 7075 aluminum. To characterize the impact, a test series was developed to calculate forces that had different impact speeds and attack angels. Attack angles were defined to be the angle between the travel of the hailstone and the surface of the plate as shown in Figure 4.

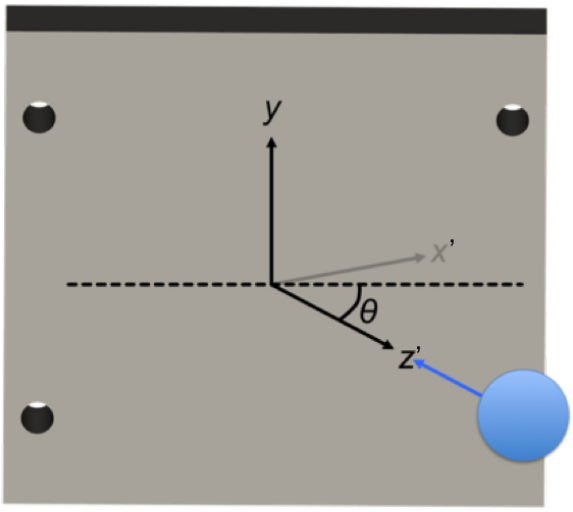

Figure 4: Diagram of how the angle of attack was defined

The hailstones were made and shot per ASTM F320-10 [1]. The stones were cast into spheres with a nominal 0.8" diameter. At this size, the stones were to have a nominal weight of 4.38 grams. They were cast by soaking a small cotton ball with water and placing it in the casting and filling up the rest of the cavity with water.

The hailstone was propelled by shooting a hail stone/pusher assembly out of a gun with gunpowder. After the assembly was shot out of the gun, the pusher would separate from the hail stone and hit a stripper plate. The hail stone would continue flying and hit the instrumented aluminum plate that was suspended from bungees. A photo of this aluminum plate can be seen in Figure 1. High Speed (HS) video was taken of the hail stones hitting the plate and the camera was set up next to the instrumented plate to capture the video. A photo of the stripper plate and the overall setup can be seen in Figure 5. SWAT-TEEM was then used on the plate to calculate the force and moments that the hail stone imparted on the plate.

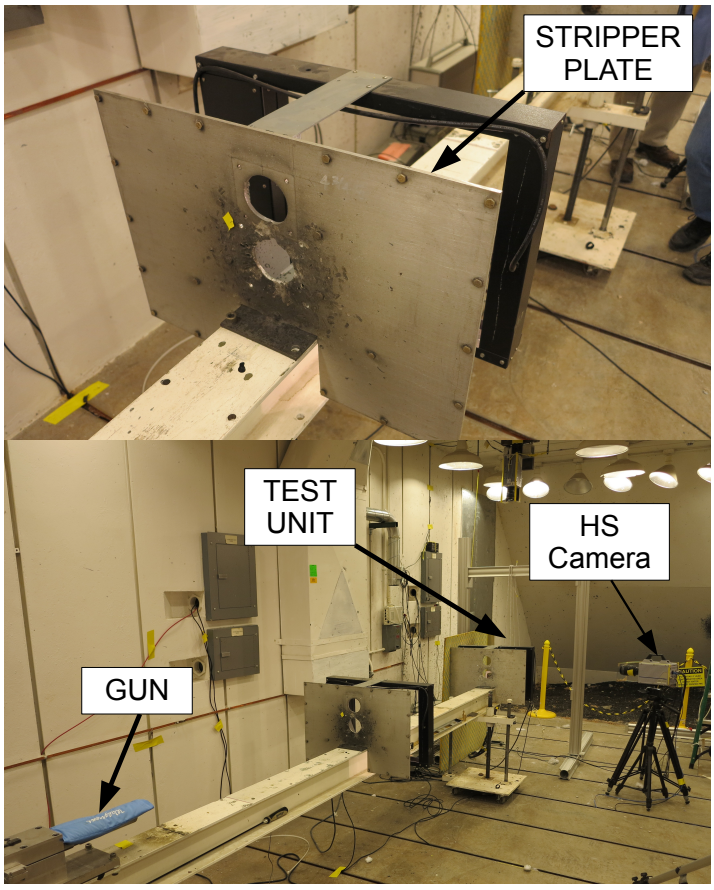

Figure 5: Photo of the Terminal Ballistics Facility setup with stripper plate (top) and overall setup (bottom)

To measure the accelerations of the nodes of the plate during the hail impact environment, Endevco 7270A-M6 20k gauges were screwed into tapped holes on the back side of the plate. A photo of one of these gauges can be seen in Figure 6. These gauges were chosen because they had a high dynamic range and were mechanically isolated which aided in suppressing the internal resonance. A photo of the plate suspended with all of the accelerometers installed can be seen in Figure 1.

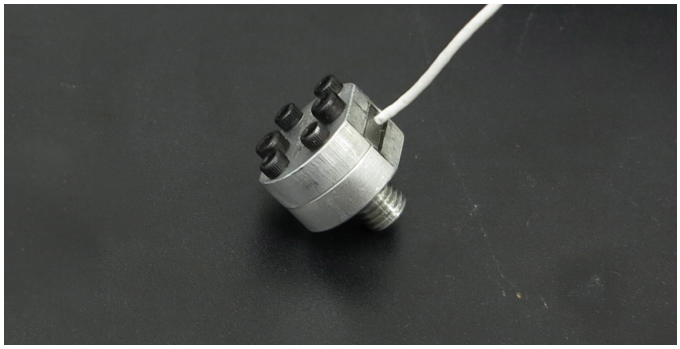

Figure 6: Photo of a Endevco 7270A-M6 20k gauge

Results

The final test matrix can be seen in Table 2. Table 2 included information on the angle of attack as defined in Figure 4, the measured speed of the hail stone per run, the measured mass of the hail stone per shot, and the magnitude of hail stone's kinetic energy as defined by

$$|KE| = \frac{(mass) \times (speed)^2}{2}. \tag{19}$$

Table 2: Actual test series for characterizing hail impact forces

Run Number	Angle	Speed $\left(\frac{\text{meter}}{\text{sec}}\right)$	Hail Mass (grams)	Kinetic Energy (J)
6	10°	286	4.29	176
7	10°	272	4.22	156
9	10°	246	4.18	127
11	10°	231	4.31	115
17	10°	506	4.20	537
20	10°	627	4.34	853
22	10°	605	4.28	784
23	10°	639	4.20	858
24	10°	677	4.36	1000
25	10°	582	4.26	721
26	10°	482	4.18	486
27	10°	484	4.27	500
32	45°	252	4.19	133
33	45°	237	4.18	117
34	45°	271	4.41	162
35	45°	526	4.46	616
38	45°	534	4.24	605
40	90°	253	4.33	140
41	90°	263	4.31	149
42	90°	272	4.43	164
43	90°	162	4.39	57
44	90°	150	4.45	50
49	90°	200	4.27	86
50	90°	365	4.41	294

For each of the runs listed in Table 2, the force in the Z direction, moment about the X axis and moment about the Y axis were calculated with SWAT-TEEM. After examination of the forces in the frequency domain, it was determined that the algorithm was only accurate to 9000 Hz and a lowpass filter was applied that had a cutoff frequency of 9000 Hz. This was due to a resonance at 10 kHz not being filtered out by SWAT-TEEM. This filtered frequency was consistent with the results from the characterization test.

Because the translational force in the Z direction and moments about the X and Y axis were measured, the location of the hail impact was calculated as it was in the characterization test. This calculation was done at time of the peak force. This result was then checked against video taken of the hail strike. A grid was drawn on the plate to aid with locating the actual impact location. A sample of snapshots of a video can be found in Figure 7.

The comparison between all of the calculated and measured locations of impact were documented and can be found in Table 3. Table 3 gives the X and Y coordinates of the calculated and measured impact locations for all of the successful impacts from Table 2.

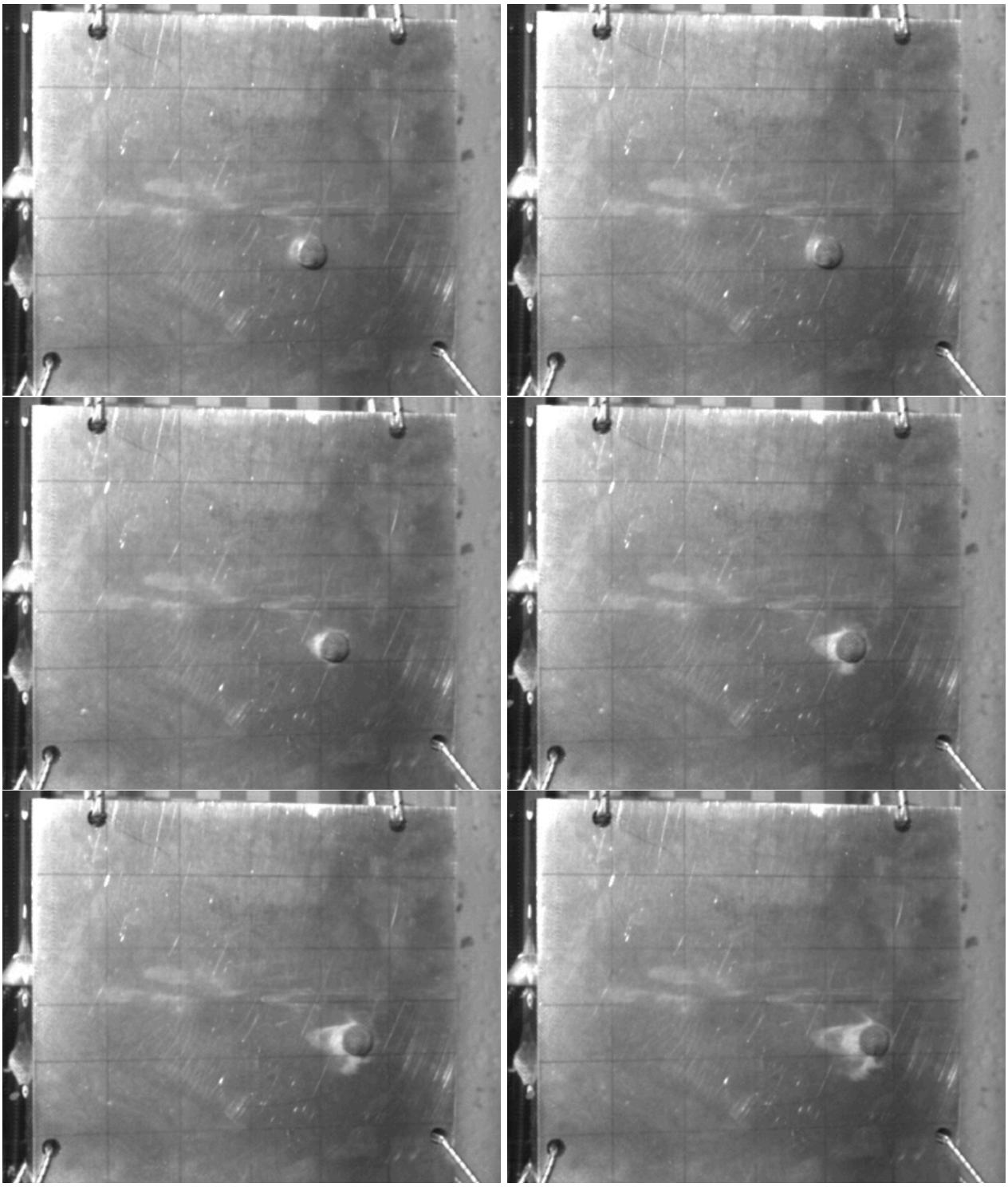

Figure 7: Still frames of Run 11 (time step of 33.3 microseconds)

Table 3: Comparison between hail impact location determined by SWAT-TEEM and high speed video

Run Number	Difference between Video and SWAT-TEEM	
	Δ X Direction (in)	Δ Y Direction (in)
6	0.0	0.1
7	0.0	0.3
9	0.0	0.1
11	0.1	0.4
17	0.1	0.9
20	0.5	0.1
22	0.2	0.2
23	0.3	0.3
24	0.5	0.5
25	0.4	0.8
26	0.3	0.2
27	0.4	0.2
32	0.0	0.2
33	0.3	0.7
34	0.3	0.3
35	0.0	0.3
38	0.9	0.9
40	0.1	0.3
41	0.2	0.1
42	0.1	0.4
43	0.2	0.4
44	0.0	0.3
49	0.3	0.4
50	0.2	0.1

The forces calculated with a 9 kHz low pass filter were concatenated into plots with respect to the impact angle. These results can be found in Figures 8, 9, and 10. It was noted that there was significant filter ring for all the shots except the low energy ten degree shots where most of the energy was contained under 9 kHz.

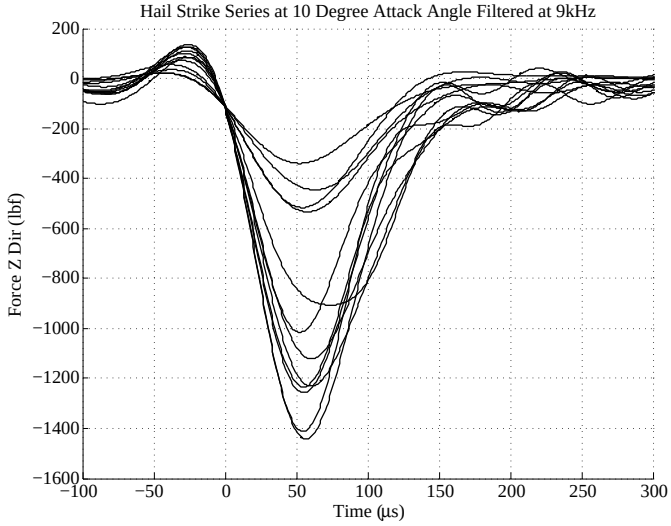

Figure 8: Summary of the forces in the time domain with a 10 degree impact angle

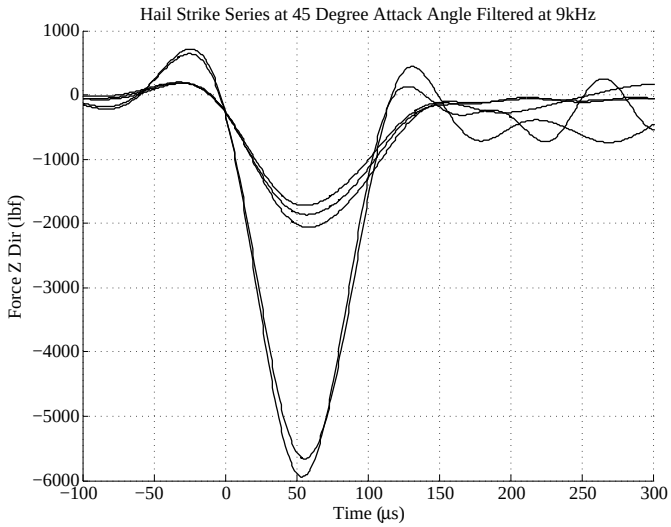

Figure 9: Summary of the forces in the time domain with a 45 degree impact angle

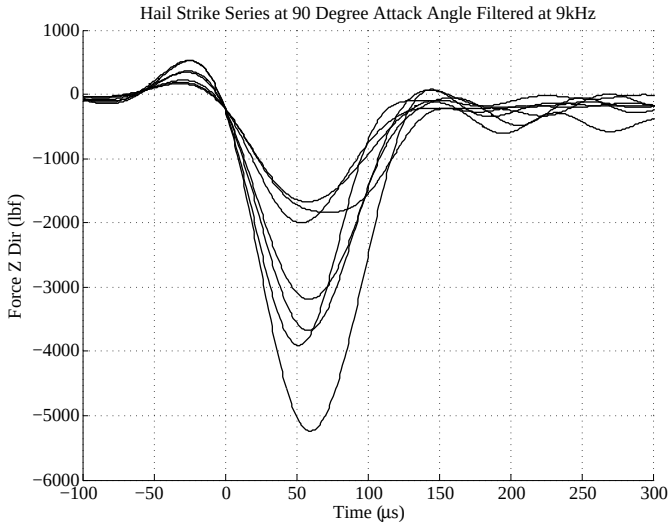

Figure 10: Summary of the forces in the time domain with a 90 degree impact angle

The peak force of the impact was also analyzed with respect to the kinetic energy of the hail stone. Figure 11 displays all of the shots with the peak force as a function of the kinetic energy of the hail stone. The figure also contains linear regression lines that were fit to each of the impact angles. It can be seen in Figure 11 that there was more variability shot to shot for the 10° impact angle shots, however, the trends for every angle of attack appeared to be linear.

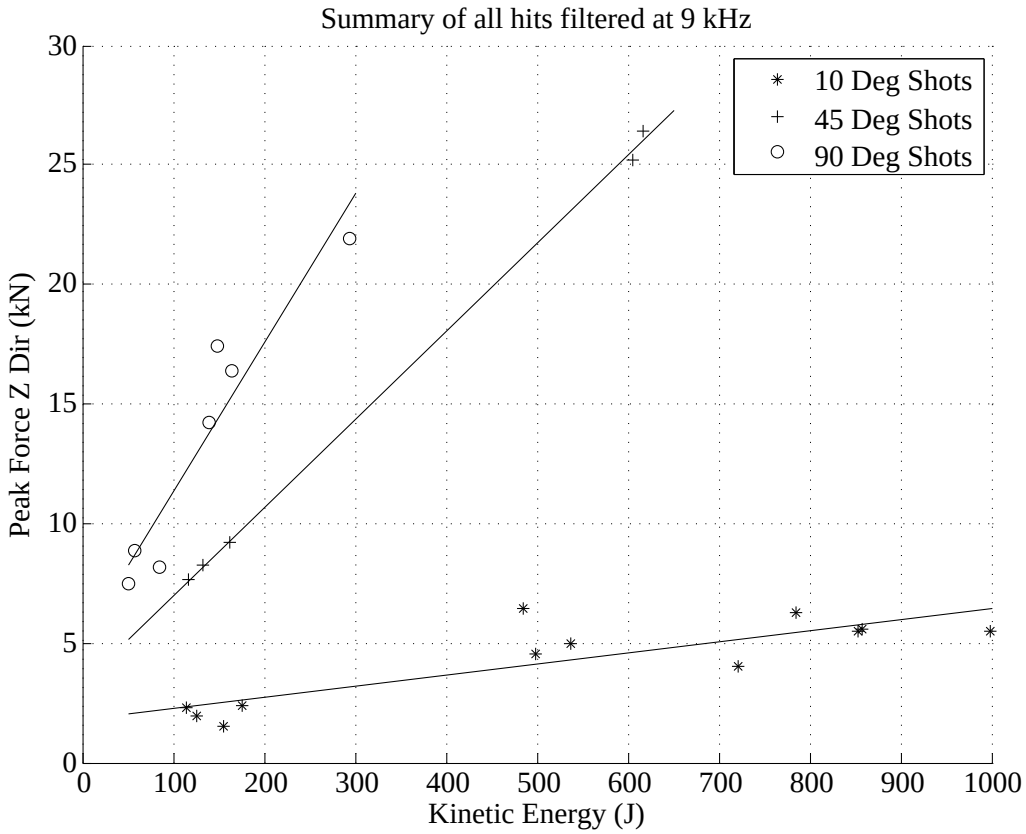

Figure 11: Characterization of peak force with respect to kinetic energy of all runs

Higher speed shots were planned for attack angles of 45 and 90 degrees. However, the Endevco 7270A-M6 20k gauges began to overload due to their internal resonances being excited from the high frequency input from the hail stone traveling at high speeds and the impulse being shorter. Figure 12 shows the frequency responses of the accelerometers from Run 50 which shows significant energy at the internal resonance frequencies. The fact that the internal resonances were excited was significant because the M6 configuration of the 7270 was mechanically isolated so that the internal resonances weren't supposed to be excited as much as the original configuration.

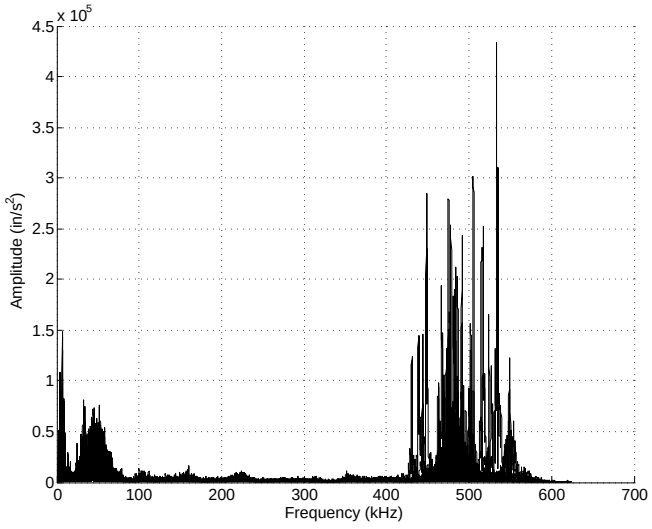

Figure 12: Frequency domain of accelerometers for Run 50 displaying the internal resonances

Conclusions and Future Work

The characterization test showed the useful bandwidths of the SWAT and SWAT-TEEM algorithms for the accelerometer configuration was 9000 Hz for SWAT-TEEM and 4000 Hz for SWAT. The characterization test also revealed that the SWAT-TEEM algorithm had a superior frequency response for the hail impact test.

Man-made hail stones were created and shot at an aluminum plate. The forces caused by the hail impacts were calculated through the SWAT-TEEM algorithm. The forces were filtered at 9000 Hz due to the limitation of the measured degrees of freedom spanning the space of the mode shapes outside that bandwidth.

Forces were calculated for hail impacts at different angles and speeds. The speeds ranged from around 152 m/s to 671 m/s. The angle of attacks were measured from the plane of the plate and were 10°, 45° and 90° (normal). The kinetic energy in the Z direction was calculated for each shot and was plotted with respect to the peak force that it caused. This relationship showed to be linear for each angle of attack.

It was determined after the test that a variety of speeds would have been useful so that more statistics could be performed on the linearity of the relationship between the kinetic energy of the hail stones versus the peak force applied.

The analysis throughout this paper calculated three of the six degree of freedom forces, translation in the Z direction, moment about the X axis and moment about the Y axis. With the proper instrumentation, all six rigid body forces could had been measured. This would had provided the friction component of the impact for the non-normal impacts.

Due to the internal resonances being excited in the accelerometers, data was not taken on the high speed large angle setups. Gauges that had more damping on its natural frequency should have been used so that data could have been acquired.

References

[1] ASTM Standard F320-10 (2010). Standard test method for hail impact resistance of aerospace transparent enclosures. ASTM International, West Conshohocken, PA, 2010, DOI: 10.1520/F0320-10. http://www.astm.org.

[2] T.G Carne, V.I. Bateman, and C.R. Dohrmann. Force reconstruction using the inverse of the mode-shape matrix. Technical Report SAND90–2737, Sandia National Laboratories, 1990.

[3] D.L. Gregory, T.G. Priddy, and D.O. Smallwood. Experimental determination of the dynamic forces acting on non-rigid bodies. *SAE Technical Paper Series, Paper No. 861791, Aerospace Technology conference and Exposition, Long Beach, CA*, October 1986.

[4] Daniel P. Hensley and Randy L. Mayes. Extending smac to multiple references, proceedings of the 24^{th} International Modal Analysis Conference. pages 220–230, January 2006.

[5] Hyonny Kim, Douglas A Welch, and Keith T Kedward. Experimental investigation of high velocity ice impacts on woven carbon/epoxy composite panels. *Composites Part A: Applied Science and Manufacturing*, 34(6):25–41, 2003.

[6] Randy L. Mayes. Measurement of lateral launch lads on re-entry vehicles using swat, proceedings of the 12^{th} International Modal Analysis Conference. pages 1063–1068, Feburary 1994.

[7] J.M. Pereira, S.A. Padula, D.M. Revilock, and M.E. Melis. Forces generated by high velocity impact of ice on a rigid structure. Technical Report NASA/TM-2006-214263, National Aeronautics and Space Administration, 2006.

[8] Jeffery D. Tippmann, Hyonny Kim, and Jennifer D. Rhymer. Experimentally validated strain rate dependent material model for spherical ice impact simulation. *International Journal of Impact Engineering*, 57:43 – 54, 2013.